Journal of Computational and Applied Mathematics 25 (1989) 277–287
North-Holland

Secondary bifurcations in the buckling problem *

C.-S. CHIEN
Department of Applied Mathematics, National Chung Hsing University, Taichung, Taiwan, 40227 R.O.C.

Received 4 February 1988
Revised 29 August 1988

Abstract: The secondary bifurcation points and secondary states of a thin plate buckling problem are numerically studied in this paper. The continuation methods and local perturbation techniques are successfully implemented to trace the first few secondary branch solutions. Our computer graphic output shows that the secondary branch process is an unsymmetric wrinkling.

Keywords: Continuation methods, buckling problem, secondary bifurcations.

1. Introduction

Consider the buckling problem

$$\begin{aligned} &\Delta u + \lambda \sin u = 0 \quad \text{in } \Omega, \\ &u = 0 \quad \text{on } \partial\Omega, \end{aligned} \tag{1.1}$$

where $\Omega \subset \mathbb{R}^n$ with $n \leqslant 3$ is a compact domain with piecewise smooth boundary $\partial\Omega$. The purpose of this paper is to study the secondary bifurcation points of (1.1) and the branch solutions emanating from these points numerically.

Equation (1.1) is of the following general nonlinear operator equation type:

$$F(u, \lambda) = 0. \tag{1.2}$$

Here $F: B_1 \times \mathbb{R} \to B_2$, $u \in B_1$, $\lambda \in \mathbb{R}$ is a smooth mapping, B_1 and B_2 are two real Banach spaces, and $\mathbb{R}$ is the real line.

A solution u_0 of (1.2) is said to be a basic solution or trivial solution if $F(u_0, \lambda) = 0$ for all values of λ. A bifurcation point on the basic solution is called a primary bifurcation point. The solutions that branch from these points are called primary branch solutions or primary states. Any solutions other than the basic solution which bifurcate from a primary state are called secondary branch solutions, and the corresponding bifurcation points are called secondary bifurcation points. We refer to [7] for details.

The earliest discovery of secondary bifurcation was made by Poincaré in his classical work on the ellipsoidal figures of equilibrium of a rotating and inviscid fluid. Secondary bifurcation was

* This work was supported by the National Science Council of Republic of China through Grant NSC77-0208-M005-04.

observed by Bauer and Reiss in their numerical study of the compressive buckling of rectangular plates, see [6,7] and the references cited in [7]. In our numerical experiments for [2,11], we also observed that secondary bifurcations exist on certain primary states of the discretizations of (1.1).

To follow a secondary branch solution emanating from a primary one numerically by the continuation method, it is necessary to first discretize the differential equation, for example, by the finite differences of the finite element method. Next we detect the primary bifurcation point along the trivial solution. The continuation methods (see [1,4,5]) and local perturbation techniques developed in [2] will then be implemented to trace the primary branch solutions and simultaneously detect the secondary bifurcation points on them. If a secondary bifurcation point is signaled, one then determines its approximate location and applies the previous perturbation techniques by choosing an appropriate perturbation vector d for the secondary branch solution. The continuation methods are used to follow the secondary branch solution again.

But it is possible that a secondary bifurcation point might be very close to the trivial solution. In this case it would be difficult to perform two consecutive different perturbations in a small interval. Thus one might perform one local perturbation for the secondary branch solution. By doing this one switches from the trivial solution directly to the secondary branch solution without passing through the primary one.

We should emphasize here that the choice of the perturbation vector d plays a key role in the numerical methods described above. It might be effective if one knows the oscillation of the eigenfunction that is corresponding to the eigenvalue where the branch bifurcates off. In this case one chooses d so that it has the same sign pattern as that of the corresponding eigenvector, see [2,11]. But the eigenfunctions of a nonlinear eigenvalue problem are in general unknown. Under such circumstances one might choose d by exploiting the symmetry of the domain Ω if possible, see [3].

Since the theoretical results concerning secondary bifurcations of (1.1) are not well understood, it is difficult to choose d for performing local perturbation. In [9,10] Cheo and Reiss established numerically that the secondary bifurcation of the uniformly compressed circular plate about an axisymmetric primary state is an unsymmetric wrinkling. These results might be helpful for us to choose the perturbation vector d. Actually our numerical results show that the secondary branching process of (1.1) is an unsymmetric wrinkling.

This paper is organized as follows. In Section 2 we briefly review the numerical methods that are required in our numerical experiments, see [2]. The numerical reports based on very coarse grids are given in Section 3. In Section 4 we employ more mesh points to get better approximations for the branch solutions of (1.1). These numerical results are illustrated by 3D computer graphs. Some comments and conclusions are also given in Section 4.

2. Tracing secondary bifurcations

2.1. Basic theory

To solve (1.1) numerically, we first discretize it, e.g., by the finite difference method. The finite dimensional approximation of (1.1) is given by

$$H(x, \lambda) = 0, \tag{2.1}$$

where $H: \mathbb{R}^N \times \mathbb{R} \to \mathbb{R}^N$, $x \in \mathbb{R}^N$, $\lambda \in \mathbb{R}$ is a smooth mapping. Thus, one can easily apply the predictor-corrector type continuation methods described below to follow the solution curves of (2.1).

Assume that 0 is a regular value of H. It is well known that $H^{-1}(0)$ is a 1-dimensional manifold which is the disjoint union of smooth curves $c(s)$ which are diffeomorphic to some interval $I \subset \mathbb{R}^1$ or to a circle S^1. We denote $c(s)$ by

$$c = \{ y(s) = (x(s), \lambda(s)) \mid H(y(s)) = 0,\ s \in I \}. \tag{2.2}$$

Differentiating $H(y(s)) = 0$ with respect to s, we obtain

$$DH(y(s)) \cdot \dot{y}(s) = 0. \tag{2.3}$$

Here $\dot{y}(s) = (\dot{x}(s), \dot{\lambda}(s))$ denotes a tangent vector to c at $y(s)$, and $DH(y(s)) = (D_x H(y(s)), D_\lambda H(y(s)))$ is the $N \times N+1$ Jacobian matrix of rank N. It follows from (2.3) that the augmented Jacobian matrix

$$A(y(s)) = \begin{bmatrix} DH(y(s)) \\ \dot{y}(s)^{\mathrm{T}} \end{bmatrix} \tag{2.4}$$

is nonsingular for all $s \in I$. If an orientation is given, and a starting point $y(0) = (x(0), \lambda(0))$ is known, then one can numerically trace c by solving the Davidenko initial-value problem (see [14,15])

$$\text{(D)} \qquad \begin{aligned} &DH(y(s)) \cdot \dot{y}(s) = 0, \\ &\| \dot{y}(s) \| = 1, \\ &y(0) = (x(0), \lambda(0)). \end{aligned}$$

Suppose that $y_i = (x_i, \lambda_i) \in \mathbb{R}^{N+1}$ has been accepted as an approximating point for c. We predict a new point $Z_{i+1,1}$ by the Euler predictor

$$Z_{i+1,1} = y_i + \delta_i \cdot u_i, \tag{2.5}$$

where $\delta_i > 0$ is the step length, and u_i is the unit tangent vector at y_i, which is obtained either by solving the linear system (see [1,4,18])

$$A(y_i) \cdot u_i = \begin{bmatrix} \bar{0} \\ 1 \end{bmatrix} \tag{2.6}$$

or

$$\begin{bmatrix} DH(y_i) \\ e_k^{\mathrm{T}} \end{bmatrix} \cdot u_i = \begin{bmatrix} \bar{0} \\ 1 \end{bmatrix}, \tag{2.7}$$

where e_k is the kth standard basis vector of $\mathbb{R}^{N+1}$ such that

$$| e_k^{\mathrm{T}} \cdot u_{i-1} | = \max \{ | e_j^{\mathrm{T}} \cdot u_{i-1} |,\ j = 1, \ldots, N+1 \}.$$

In order to maintain orientation and control the local curvature, we impose the following condition:

$$u_i \cdot u_{i-1} > 1 - \alpha > 0 \quad \text{for some } \alpha \in (0, 1). \tag{2.8}$$

The accuracy of approximation to the solution curve $c(s)$ is in general improved by a corrector process. This is done by choosing a hyperplane which is orthogonal to $\dot{y}(s)$ at $Z_{i+1,1}$ and performing Newton iterations constraint to the hyperplane. In practice, the modified Newton's method with constraint

$$\begin{bmatrix} DH(Z_{i+1,1}) \\ \gamma^{T} \end{bmatrix} \cdot w_j = \begin{bmatrix} -H(Z_{i+1,j}) \\ 0 \end{bmatrix}, \quad j = 1, 2, 3, \ldots, \tag{2.9}$$

is solved, where the predictor point $Z_{i+1,1}$ is used as the initial guess, and $Z_{i+1,j+1} = Z_{i+1,j} + w_j$, $j = 1, 2, 3, \ldots$. Two possible choices for the constraint vector γ are

(i) the current unit tangent vector u_i,

(ii) the standard base e_k of $\mathbb{R}^{N+1}$ defined in (2.7).

If y_i lies sufficiently near c, then the Newton iteration (2.9) will converge provided the step size $\delta_i > 0$ is small enough.

One can solve (2.6) (or (2.7)) and (2.9) either by direct methods or iterative methods. The direct methods are used in our numerical experiments. The reason is that no extra computation is necessary for detecting bifurcation points.

The predictor-corrector type continuation methods can be used to follow the secondary bifurcation curves as well as the primary bifurcation curves. Before doing this, we have to detect secondary bifurcations on the primary bifurcating solutions.

2.2. Detecting secondary bifurcations

The numerical methods we developed in [2] can be used to detect both bifurcations and secondary bifurcations regardless of the multiplicities. The theoretical foundation is based on a result of Berger [8]: if F is an odd gradient map with respect to u and $DF(u(s^*), \lambda(s^*))$ has rank deficiency m, then at least m branches bifurcate from c at $(u(s^*), \lambda(s^*))$. In the finite dimensional context, in order for Berger's result to apply, $D_x H$ should be symmetric and $D_x H(-x, \lambda) = -D_x H(x, \lambda)$ should hold.

Actually under the above hypotheses, our criterion can be viewed as an extension of the classical criterion based on a theorem of Crandall and Rabinowitz [13], which is applicable only when the bifurcation is odd, even without knowing its multiplicities, see [1,2,14,15] for details. For completeness, we briefly review our bifurcation criterion given in [2].

Let A be a symmetric $N \times N$ matrix, and let $p(A)$, $n(A)$ denote the number of positive and negative eigenvalues of A, respectively. The number $\sigma(A) = p(A) - n(A)$ is called the signature of A. Sylvester's Law of Inertia states that $\sigma(PAP^{T}) = \sigma(A)$ and

$$p(PAP^{T}) = p(A) \tag{2.10}$$

whenever P is a nonsingular matrix, see [17]. Since the reduction of $D_x H$ to an upper triangular matrix may be represented by $PD_x HP^{T}$ for some nonsingular matrix P, we may detect bifurcations in the course of following c via the above sketched numerical continuation process. Let y_i and y_{i+1} be two consecutive approximations to c such that only one singular point of $D_x H$ lies on c between them. Suppose that

$$| p(D_x H(y_{i+1})) - p(D_x H(y_i)) | = m. \tag{2.11}$$

Then exactly m eigenvalues of $D_x H(y(s))$ change sign at some point $y^* = y(s^*)$ approximately between y_i and y_{i+1}. By the abovementioned result of Berger, if $D_x H(x, \lambda)$ is odd in x, then at

least m branches bifurcate from c at $y(s^*)$. Furthermore, the precise difference in signature (2.11) can be easily detected, since it is equal to change in signature of the corresponding diagonalized matrices

$$\left| p\left(P_{i+1} D_x H(y_{i+1}) P_{i+1}^{\mathrm{T}}\right) - p\left(P_i D_x H(y_i) P_i^{\mathrm{T}}\right) \right|. \tag{2.12}$$

We remark here that no extra computation is required for our numerical methods if the direct methods are implemented to solve (2.6) or (2.7). It is obvious that Berger's result can be applied to the discretization (1.1).

2.3. Perturbation for secondary bifurcations

Local perturbation techniques can be used to handle both simple and multiple bifurcations. Our numerical experiments given in Section 3 show that this is also true for secondary bifurcations. The theoretical foundation of local perturbation is based on a version of generalized Sard's theorem. The implementation of local perturbation for bifurcation can be found, e.g., in [2,3,11,14,15]. We will briefly review them.

Theorem 2.1. *Let $V \subset \mathbb{R}^m$, $W \subset \mathbb{R}^p$ be nonempty open sets and let $\phi : V \times W \to \mathbb{R}^n$ be a smooth map with $m \geqslant n$. If 0 is a regular value of ϕ, then for almost all $d \in W$, 0 is a regular value of the restricted map $\phi_d(\cdot) = \phi(\cdot, d)$.*

For our particular application of the above theorem, we set $m = N + 1$ and $p = N$. Now suppose that $y(s^*)$ is a detected bifurcation point on the curve $c \subset H^{-1}(0)$. Let $U \subset \mathbb{R}^{N+1}$ be a bounded open neighborhood of $y(s^*)$. Let $f : \mathbb{R}^{N+1} \to \mathbb{R}$ be a smooth map such that $f(y) = 0$ for $y \notin U$ and $f(y) > 0$ for $y \in U$. The following result (see [14]) is used in our practical computation.

Lemma 2.2. *For H, U, f defined as above, let $H_d : \mathbb{R}^{N+1} \to \mathbb{R}^N$ be defined by*

$$H_d(y) = H(y) + f(y) d. \tag{2.13}$$

Then $H_d(y)$ has 0 as a regular value for almost all $d \in \mathbb{R}^N - \{0\}$.

One can easily choose the perturbation vector d if the oscillation of the components of the solution branch is known. Note that the latter is in general reflected by the components of the associated eigenfunction, see [2]. Although the behavior of the secondary bifurcations of the buckling problem is still unknown, we can choose suitable perturbation vectors for the first few secondary bifurcations, since the oscillations of the components of these secondary bifurcations are so natural. Our numerical experiments given below will confirm this aspect.

3. Numerical results

The eigenvalues and corresponding eigenfunctions of the linear problem

$$\begin{aligned} &\Delta u + \lambda u = 0 \quad \text{in } \Omega = (0, 1)^2, \\ &u = 0 \qquad\quad \text{on } \partial\Omega, \end{aligned} \tag{3.1}$$

are known to be

$$\lambda_{m,n} = (m^2 + n^2)\pi^2, \tag{3.2}$$

$$u_{m,n}(x, y) = \pm \sin m\pi x \cdot \sin n\pi y, \tag{3.3}$$

for $m, n = 1, 2, 3, \ldots$.

If $m = n$, then $\lambda_{m,n}$ is a simple eigenvalue, whereas if $m \neq n$, then $\lambda_{m,n}$ is at least a double eigenvalue.

The eigenvalues and corresponding eigenvectors of the standard five-point centered difference analogue of (3.1) are given by

$$\mu_{p,q} = 4\left[(J+1)^2 \sin^2 \tfrac{1}{2}\pi\left(\frac{p}{J+1}\right) + (K+1)^2 \sin^2 \tfrac{1}{2}\pi\left(\frac{q}{K+1}\right)\right], \tag{3.4}$$

$$U_{p,q}(x_j, y_k) = \sin\left(\frac{jp\pi}{J+1}\right) \sin\left(\frac{kq\pi}{K+1}\right), \tag{3.5}$$

where J and K are the number of interior nodes on the x- and y-axis, respectively, and $(x_j, y_k) = (j/(J+1), k/(K+1))$, $1 \leqslant j, p \leqslant J$, $1 \leqslant k, q \leqslant K$, see [16].

Since the linearization about the trivial solution of the buckling problem

$$\begin{aligned} &\Delta u + \lambda \sin u = 0 \quad \text{in } \Omega = (0, 1)^2, \\ &u = 0 \qquad\qquad\quad \text{on } \partial\Omega, \end{aligned} \tag{3.6}$$

is the linear problem (3.1), it is obvious that the eigenvalues of (3.6) would be the same as those of (3.1). Similar results also hold for those of the discretizations of (3.6) and (3.1).

The central difference approximation of (3.6) is given by

$$\begin{aligned} &\Delta U_h + \mu \sin U_h = 0 \quad \text{in } \Omega = (0, 1)^2, \\ &U_h = 0 \qquad\qquad\quad \text{on } \partial\Omega. \end{aligned} \tag{3.7}$$

Here $h = 1/(N+1)$ with N a positive integer is the uniform meshsize on the x- and y-axis. The standard serpentine ordering of interior nodal points is used. That is, $U(x_j, y_k)$ is relabeled as U_l, $l = j + (N-1)k$. The accuracy tolerance is $5.0 \cdot 10^{-4}$ throughout the experiments given in this paper. As we mentioned in Section 1, the secondary bifurcations of (3.6) are not well understood. In order to make the choice of the perturbation vector d easier, our numerical experiments are first performed on very coarse grids. It is not surprising that the branch solutions of (3.7) obtained in this case are not accurate approximations for those of (3.6).

For $J = K = 3$ and $h = \frac{1}{4}$ one easily computes the eigenvalues of (3.7) by (3.4). The primary states of (3.7) branch off from the trivial solution $U_h \equiv 0$ precisely at the location of the eigenvalues, see [20]. The location of all the eigenvalues of (3.7) with $h = \frac{1}{4}$ is given in Fig. 1. Note that these eigenvalues are all equally spaced.

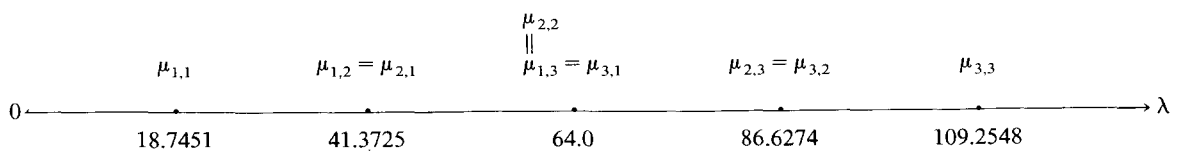

Fig. 1.

Let A be the 9×9 matrix associated with (3.7). As we trace along the trivial solution $U_h \equiv 0$ of (3.7), the signature jump of A is 0, 1, 3, 6, 8, 9, respectively, whenever each eigenvalue is passed. That is, $\mu_{1,1}$ and $\mu_{3,3}$ are simple eigenvalues, $\mu_{1,2} = \mu_{2,1}$ and $\mu_{2,3} = \mu_{3,2}$ are double eigenvalues, while $\mu_{1,3} = \mu_{3,1} = \mu_{2,2}$ is a triple eigenvalue. The associated branch curves have been investigated in [2]. We will be interested only in secondary bifurcations.

There is no secondary bifurcation on the branch curve bifurcating at the first simple eigenvalue $\mu_{1,1} \cong 18.7451$. The signature of A jumps from 1 to 2 between $\mu \cong 41.19$ and 41.67 on each of the two primary branch curves bifurcating at $\mu_{1,2} \cong \mu_{2,1} \cong 41.3725$, where $\| U_h \|_\infty \cong 0.09$. This shows that a simple secondary bifurcation indeed exists on each of these two branch curves, and these two secondary bifurcations are very close to the double bifurcation $\mu_{1,2} = \mu_{2,1}$.

To obtain these two secondary branch curves, we start from the trivial solution $U_h \equiv 0$, and perform local perturbation near the secondary bifurcation points by choosing the perturbation vectors d so that the components $d_l = 0$ on each of the diagonals. The other components of d are chosen so that d_l's have different signs on each of the subregions divided by the diagonals. Note that we set $\| d \|_\infty = 10^{-3}$.

At $\mu = 43.80$ the two primary branch solutions are (0.487, 0.667, 0.487, 0, 0, 0, −0.487, −0.667, −0.487) and (−0.487, 0, −0.487, −0.667, 0, −0.667, −0.487, 0, −0.667), respectively. It is obvious that the nodal sets (see [12]) of these two primary states lie on the respective line segments connecting (0, 0.5), (1, 0.5) and (0.5, 0), (0.5, 1). The nodal set of one of the secondary branch curves is on the diagonal connecting (0, 0) and (1, 1), while the other is on the diagonal connecting (0, 1) and (1, 0). At $\mu = 43.80$ these two secondary states are (0, −0.487, −0.667, 0.487, 0, −0.487, 0.667, 0.487, 0) and (−0.667, −0.487, 0, −0.487, 0, 0.487, 0.667).

The signature of A jumps from 3 to 4 between $\mu = 63.99$ and 64.29 as we follow the branch curve bifurcating at $\mu_{2,2} = \mu_{1,3} = \mu_{3,1}$ which is associated with $\mu_{2,2}$, where $\| U_h \|_\infty \cong 0.137$. That is, a simple secondary bifurcation is signaled on this branch curve, and this simple secondary bifurcation is close to the triple bifurcation.

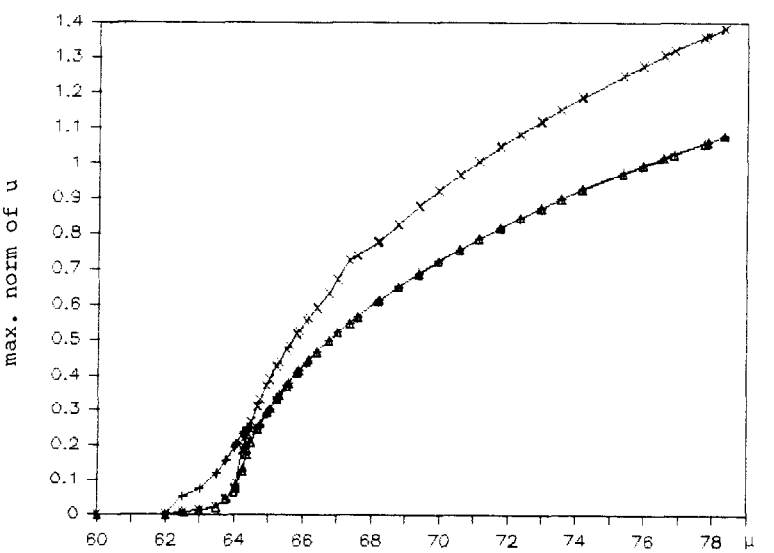

Fig. 2. Bifurcation at $\mu_{2,2}$ and secondary bifurcation. × double, Δ simple, + secondary.

We start from the trivial solution $U_h \equiv 0$ where μ is close to this triple bifurcation point, and perform local perturbation near this triple bifurcation. It is quite natural that we choose the perturbation vector d so that $d_l = 0$ on the nodes that lie on the two diagonals of the unit square. The nodal set of the branch curve associated with $\mu_{2,2}$ lies on the two line segments connecting (0, 0.5), (1, 0.5) and (0.5, 0), (0.5, 1). It is not surprising that the nodal set of this secondary branch curve lies on the two diagonals. The solutions of the primary state and the secondary state at $\mu = 65.81$ are (0.408, 0, −0.408, 0, 0, 0, −0.408, 0, 0.408) and (0, 0.408, 0, −0.408, 0, −0.408, 0, 0.408, 0), respectively. Figure 2 shows that the primary branch solutions bifurcate at $\mu_{1,3} = \mu_{3,1}$ and $\mu_{2,2}$, and the secondary branch solution emanates from the latter.

The signature of A jumps from 3 to 4 between $\mu = 72.97$ and 74.17 as we trace one of the primary branch curves bifurcating at $\mu_{1,3} = \mu_{3,1} = 64$. Similar result holds for the other primary state because of the conjugacy at double eigenvalues, see [19].

A secondary bifurcation point is detected between $\mu = 98.95$ and 101.3 on each of the branch curves bifurcating at $\mu_{2,3} = \mu_{3,2} \cong 86.6274$. No secondary bifurcation point has been detected yet as we trace the primary branch curve bifurcating at $\mu_{3,3} \cong 109.2548$ until $\mu = 331.8$. The numerical reports about these secondary states will not be given here.

We should emphasize here that the oscillation of the components of the primary states do not always follow (3.5). For example, the sign of the components of $U_{2,3}(x_j, y_k)$ is given by

$$\pm(+, 0, +, -, 0, +, +, 0, -).$$

But the counterparts of one of the associated primary branch curves is

$$\pm(-, +, +, +, 0, -, -, -, +).$$

4. Results on finer grids and conclusions

The numerical computations will be performed on the finer grids in this section. It follows from Lemma 2.2 in Section 2 that one might choose d at random.

With $N = 7$ and $h = \frac{1}{8}$, there is no secondary bifurcation point on the first primary state bifurcating at $\mu_{1,1} \cong 19.4867$. The secondary bifurcation points on each of the branch curves bifurcating at the multiple eigenvalue $\mu_{1,2} = \mu_{2,1} \cong 47.2335$ are simple, and detected where $\mu \in (113.0, 114.0)$ and $\mu \in (160.6, 189.4)$, etc. In order to obtain the first secondary branch curve we perform local perturbation near $\mu = 112.0$ on one of the primary state by choosing d so that the components $d_l = 0$ on the diagonal connecting (0, 0) and (1, 1). The other components of d are chosen so that d_l's have different signs on each of the subregions divided by this diagonal. Note that we set $\| d \|_\infty = 10^{-3}$. This secondary branch curve is successfully traced. Now from the computer output it is not difficult to choose d for the first secondary branch solution emanating from the other conjugate primary state. That is, one chooses d so that the sign pattern of d is similar to that of this secondary branch solution.

Figure 3 shows the 3D graph of one of the primary branch curves at $\mu \cong 127.5$ which bifurcates from the trivial solution at $\mu_{1,2} \cong 47.2335$. The graph of the other primary state can be obtained by rotating the above graph counter-clockwise about the center of 90°. It is obvious that the isotropy subgroups on the double bifurcations are conjugate, see [19,21] for details.

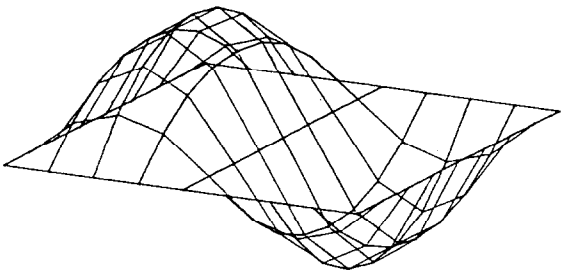

Fig. 3. 3D graph of the primary state at $\mu \cong 127.5$.

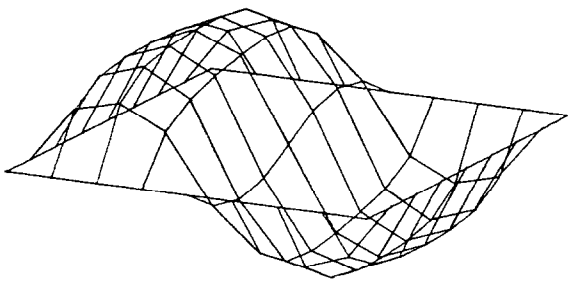

Fig. 4. 3D graph of the secondary state at $\mu \cong 127.2$.

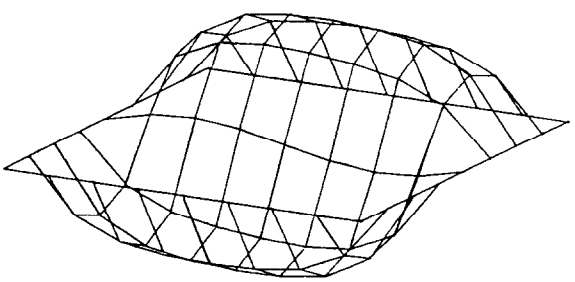

Fig. 5. 3D graph of the secondary state at $\mu \cong 127.2$.

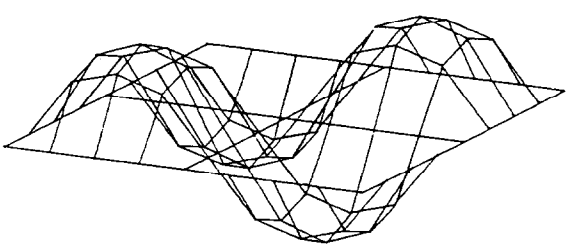

Fig. 6. 3D graph of the primary state at $\mu \cong 132.2$.

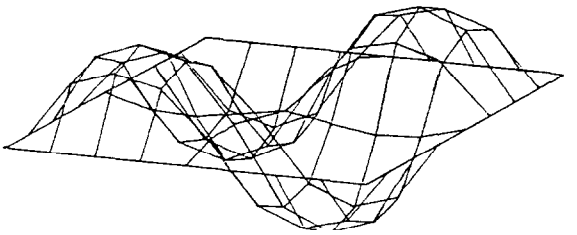

Fig. 7. 3D graph of the secondary state at $\mu \cong 132.1$.

Figures 4 and 5 show the 3D graphs at $\mu \cong 127.2$ of the two secondary branch curves, each of them bifurcates from the respective primary states at $\mu \in (113.0, 114.0)$.

The first two secondary bifurcation points on the branch curve bifurcating at $\mu_{2,2} \cong 74.9804$ are simple and detected where $\mu \in (127.8, 128.2)$ and $\mu \in (165.8, 180.2)$. Figure 6 is the 3D graph of the primary state at $\mu \cong 132.2$ which bifurcates from the trivial solution at $\mu_{2,2} \cong 74.9804$. Figure 7 shows the graph of the first secondary state at $\mu \cong 132.1$ which bifurcates from the above primary state.

The other secondary states of (1.1) of course can be numerically traced in a similar way. Now we will give some comments and conclusions about our numerical results.

From the computer graphs given in Figures 3 and 6 it is obvious that the primary states of (3.6) (or (3.7)) satisfy some symmetric properties. Actually the actions on these primary states are subgroups of the dihedral group D_4. For details we refer to [19,21], and the further references cited in [21]. Figures 4, 5 and 7 show that the secondary branching process is an unsymmetric wrinkling. To the author's knowledge, theoretical results concerning the group structures on the secondary bifurcations are not known. But from [9,10] and our numerical results it seems true that symmetry on the primary bifurcations will become unsymmetric as a secondary state branches off from the primary one.

The above numerical experiments were performed on CDC CYBER 180/830. The 3D graphs were obtained by using piecewise linear interpolation and performed on NEC PC-9801F.

Acknowledgment

This problem was originated from Prof. E.L. Allgower while the author visited him at Colorado State University in August, 1987. The author wishes to thank the anonymous referees for their valuable comments and suggestions.

References

[1] E.L. Allgower, A survey of homotopy methods for smooth mappings, in: E.L. Allgower, K. Glashoff and H.-O. Peitgen, Eds., *Numerical Solutions of Nonlinear Equations*, Lecture Notes in Math. **878** (Springer, Berlin, 1981) 1–29.

[2] E.L. Allgower and C.-S. Chien, Continuation and local perturbation for multiple bifurcations, *SIAM J. Sci. Stat. Comput.* **7** (1986) 1265–1281.

[3] E.L. Allgower, C.-S. Chien and K. Georg, Large sparse continuation problems, *J. Comput. Appl. Math.* **26** (1&2) (1989), to appear.

[4] E.L. Allgower and K. Georg, Simplicial and continuation methods for approximating fixed points and solutions to systems of equations, *SIAM Rev.* **22** (1980) 25–86.
[5] E.L. Allgower and K. Georg, Predictor-corrector and simplicial methods for approximating fixed points and zero points of nonlinear mapping, in: A. Bachem, M. Grotschel and B. Korte, Eds., *Mathematical Programming: The State of the Art* (Springer, New York, 1983) 15–56.
[6] L. Bauer and E.L. Reiss, Nonlinear buckling of rectangular plates, *J. Soc. Indust. Appl. Math.* **13** (1965) 603–626.
[7] L. Bauer, H.B. Keller and E.L. Reiss, Multiple eigenvalues lead to secondary bifurcations, *SIAM Rev.* **17** (1975) 101–122.
[8] M.S. Berger, On one parameter families of real solutions of nonlinear operator equations, *Bull. Amer. Math. Soc.* **75** (1969) 456–459.
[9] L.S. Cheo and E.L. Reiss, Unsymmetric wrinkling of circular plates, *Quart. Appl. Math.* **31** (1973) 75–91.
[10] L.S. Cheo and E.L. Reiss, Secondary buckling of circular plates, *SIAM J. Appl. Math.* **26** (1974) 490–495.
[11] C.-S. Chien, Multiple bifurcations on 3-dimensional eigenvalue problems, *Chinese J. Math.* **15** (1987) 181–194.
[12] R. Courant and D. Hilbert, *Methods of Mathematical Physics, Vol. I* (Interscience, New York, 1953).
[13] M.G. Crandal and P.H. Rabinowitz, Bifurcations from simple eigenvalues, *J. Funct. Anal.* **8** (1971) 321–340.
[14] K. Georg, On tracing an implicitly defined curve by quasi-Newton steps and calculating bifurcation by local perturbation, *SIAM J. Sci. Stat. Comput.* **2** (1981) 35–50.
[15] K. Georg, Numerical integration of the Davidenko equation, in: E.L. Allgower, K. Glashoff and H.-O. Peitgen, Eds., *Numerical Solutions of Nonlinear Equations*, Lecture Notes in Math. **878** (Springer, Berlin, 1981) 128–161.
[16] E. Isaacson and H.B. Keller, *Analysis of Numerical Methods* (Wiley, New York, 1965).
[17] L. Mirskey, *An Introduction to Linear Algebra* (Clarendon, Oxford, 1963).
[18] W.C. Rheinboldt, Numerical analysis continuation methods for nonlinear structural problems, *Comput. & Structures* **13** (1981) 103–113.
[19] D.H. Sattinger, Transformation groups and bifurcation at multiple eigenvalues, *Bull. Amer. Math. Soc.* **79** (1973) 709–711.
[20] I. Stakgold, Branching of solutions of nonlinear equations, *SIAM Rev.* **13** (1971) 289–331.
[21] I. Stewart, Bifurcation with symmetry, in: *New Directions in Dynamical Systems*, Chaos Workshop, Cambridge University, 1986.